DOI: 10.1002/cphc.200900966

Thermal Fluctuations Determine the Electron-Transfer Rates of Cytochrome c in Electrostatic and Covalent Complexes

Hoang Khoa Ly,[a] Marcelo A. Marti,[b] Diego F. Martin,[b] Damian Alvarez-Paggi,[b] Wiebke Meister,[a] Anja Kranich,[a] Inez M. Weidinger,[a] Peter Hildebrandt,*[a] and Daniel H. Murgida*[b]

The heterogeneous electron-transfer (ET) reaction of cytochrome c (Cyt-c) electrostatically or covalently immobilized on electrodes coated with self-assembled monolayers (SAMs) of ω-functionalized alkanethiols is analyzed by surface-enhanced resonance Raman (SERR) spectroscopy and molecular dynamics (MD) simulations. Electrostatically bound Cyt-c on pure carboxyl-terminated and mixed carboxyl/hydroxyl-terminated SAMs reveals the same distance dependence of the rate constants, that is, electron tunneling at long distances and a regime controlled by the protein orientational distribution and dynamics that leads to a nearly distance-independent rate constant at short distances. Qualitatively, the same behavior is found for covalently bound Cyt-c, although the apparent ET rates in the plateau region are lower since protein mobility is restricted due to formation of amide bonds between the protein and the SAM. The experimental findings are consistent with the results of MD simulations indicating that thermal fluctuations of the protein and interfacial solvent molecules can effectively modulate the electron tunneling probability.

1. Introduction

Direct electrochemistry of redox metalloproteins immobilized on electrodes coated with biocompatible or biomimetic films is an active field of fundamental and applied research. On the one hand, electrochemical and spectroelectrochemical methods can afford a great deal of information on the electron-transfer (ET) mechanisms and dynamics of the anchored protein that can contribute to the understanding of its functioning in vivo.[1–3] For instance, protein dynamics has been recently recognized as a key factor in controlling or limiting inter- and intraprotein ET reactions.[4–15] However, in most cases the complexity of the systems impairs direct observations of conformational gating, configurational fluctuations, or rearrangement of protein complexes under reactive conditions. In this context, the combination of suitable spectroelectrochemical techniques with simplified model systems, such as proteins immobilized on biomimetic electrodes, can greatly contribute to the elucidation of the biophysical fundamentals in better detail. On the other hand, the knowledge gained from these studies is essential for the rational design of protein-based technological devices such as biosensors and biofuel cells.[16–18]

The most widely used electrode coatings are self-assembled monolayers (SAMs) of single or mixed alkanethiols containing ω-functional groups that are chosen according to the protein's surface properties.[2,3] One of the specific advantages of this approach is to facilitate the determination of ET rate constants k_{ET} as a function of distance by simply varying the chain length of the thiols, as first shown by Chidsey.[19] In principle, the heterogeneous ET reaction for such systems is expected to follow a nonadiabatic mechanism, and thus its rate can be described in terms of the high-temperature limit of the semiclassical Marcus expression, integrated to account for all the electronic levels ε of the metal electrode contributing to the process [Eq. (1)]:[20]

$$k_{ET} = \frac{\pi}{\hbar}\frac{|V|^2\rho}{\sqrt{\pi\lambda k_B T}} \int_{-\infty}^{\infty} \exp\left[-\left(\frac{(\lambda + (\varepsilon_F - \varepsilon) + e\eta)^2}{4\lambda k_B T}\right)\right] \frac{1}{1+\exp[(\varepsilon-\varepsilon_F)/k_B T]}\,d\varepsilon \quad (1)$$

where $\rho(\varepsilon)$ is the density of electronic states in the electrode, and ε_F the energy of the Fermi level. The applied overpotential,

[a] H. K. Ly,[+] W. Meister, Dr. A. Kranich, Dr. I. M. Weidinger, Prof. P. Hildebrandt
Technische Universität Berlin, Institut für Chemie
Str. des 17. Juni 135, Sekr. PC14, Berlin (Germany)
Fax: (+49) 30-31421122
E-mail: hildebrandt@chem.tu-berlin.de

[b] Dr. M. A. Marti,[+] D. F. Martin,[+] D. Alvarez-Paggi, Prof. D. H. Murgida
Departamento de Química Inorgánica, Analítica y
Química Física INQUIMAE-CONICET
Facultad de Ciencias Exactas y Naturales
Universidad de Buenos Aires, Ciudad Universitaria
Pab. 2, piso 1, C1428EHA Buenos Aires (Argentina)
Fax: (+54) 11-4576-3341
E-mail: dhmurgida@qi.fcen.uba.ar

[+] These authors made equal contributions to this work and are thus listed in alphabetical order.

Supporting information for this article is available on the WWW under http://dx.doi.org/10.1002/cphc.200900966.

reorganization energy, and magnitude of the electronic coupling are denoted by η, λ, and $|V|$, respectively. The remaining parameters have the usual meaning. Equation (1) can be expressed in a simplified form by approximating the Fermi distribution law as a step function [Eq. (2)]:

$$k_{ET} \approx \frac{\pi}{\hbar}|V|^2 \rho \ \mathrm{erfc}\left(\frac{\lambda + e\eta}{\sqrt{4\lambda k_B T}}\right) \quad (2)$$

where erfc(z) is the complementary error function.

The electronic coupling $|V|$ decays exponentially with increasing separation of the redox center from the electrode, and therefore Equations (1) and (2) predict an exponential distance dependence of k_{ET}, that is, decreasing rate with increasing chain length of the alkanethiols. This prediction has been verified for a variety of redox proteins immobilized on different types of SAM-coated electrodes, including Cu_A centers, azurin, iso-cytochrome c and cytochromes c, c_6, and b_{562}, among others.[21–26] The average tunneling decay parameter β obtained for the different proteins is about 1.1 per methylene group of the thiols.

A common feature encountered for all cases studied so far is that the exponential variation of the apparent ET rate constant k_{ET}^{app} is only verified when the proteins are attached to relatively long chain tethers, usually containing nine or more methylene groups. In contrast, for thinner SAMs, k_{ET}^{app} becomes distance-independent, thus suggesting a change of the reaction mechanism. This "unusual" distance dependence has been most extensively studied for mammalian cytochrome c (Cyt-c) by several groups employing different approaches. Most of the work refers to Cyt-c electrostatically adsorbed to electrodes coated with SAMs including ω-carboxyl alkanethiols.[23,27–34] In addition, Waldeck and co-workers have studied the ET kinetics of Cyt-c coordinatively bound to electrodes coated with mixed SAMs in which one of the thiol components contained a tail group able to bind to the heme iron atom by displacing the native axial ligand Met80.[23,35–38] Both modes of immobilization yield a qualitatively similar "unusual" distance dependence of k_{ET}^{app}, although values for coordinative binding are higher due to the artificially improved electron-transfer pathway. Furthermore, in both cases the ET rates in the plateau region of the k_{ET}^{app} versus distance plots depend on the viscosity of the solution, which has been discussed controversially. Niki et al. proposed a gated mechanism based on a two-state model, in which the thermodynamically stable electrostatic complex Cyt-c/SAM represents an unfavorable configuration for ET such that protein reorientation is required to generate the electrochemically active state.[23,32] The model assumes that the rate of reorientation is distance-independent, while electron tunneling rates vary exponentially. Therefore, at sufficiently short chain lengths reorientation becomes rate-limiting and k_{ET}^{app} reaches a plateau. In contrast, based on studies of coordinatively bound Cyt-c, Waldeck et al. proposed a change from the nonadiabatic regime at long distances to the friction-controlled (adiabatic) regime at short distances,[38] which in principle could also apply to electrostatic Cyt-c/SAM complexes. Time-resolved surface-enhanced resonance Raman (TRSERR) spectroeletrochemical experiments showed that coordinative Cyt-c/SAM complexes exhibit a pronounced overpotential dependence of k_{ET}^{app} in the plateau region with a reorganization energy of 0.58 eV, and thus support the friction model.[35] For electrostatic complexes, instead, k_{ET}^{app} is nearly independent of the applied overpotential in the plateau region, and thereby points to a process other than ET that becomes rate-limiting at short distances.[3] By using Q-band excitation TRSERR[27,30] and molecular dynamics (MD) simulations,[27,39] we have provided the first direct evidence that this gating mechanism is related to protein reorientation in search of efficient electron pathways. The resulting model, however, differs from that originally proposed by Niki et al., since reorientation rates have been found to be modulated by the interfacial electric field, which in turn varies with the chain length of the SAMs. Moreover, we have shown, both experimentally[2,3,40] and theoretically,[41] that electric fields of the magnitude estimated for short SAMs as well as for biological interfaces, are able to modulate not only the ET dynamics but also the structure and function of the protein. These findings support the hypothesis that the transmembrane potential in mitochondria may regulate the ET-driven proton-pumping activity of cytochrome c oxidase (CcO) through electric field dependent interprotein ET from Cyt-c to CcO. Furthermore, the interfacial electric field may constitute the switch for the transition from the redox to the apoptotic function of Cyt-c.

In a recent electrochemical study, Davis et al. reported that the ET kinetics of Cyt-c cross-linked to mixed SAMs composed of COOH- and OH-terminated alkanethiols exhibits identical distance dependence to electrostatic complexes with the same SAMs, and is qualitatively similar to that of electrostatic complexes with pure ω-carboxyl alkanethiol SAMs.[42] Since covalent attachment is expected to restrict protein mobility, these results cast some doubts on the general validity of the electric field dependent protein-dynamics model proposed previously.[2,30]

The present work is dedicated to elucidating this contradiction. Using TRSERR and MD simulations we have performed a comparative study of the ET properties of Cyt-c in electrostatic and covalent SAM/Cyt-c complexes with single-component and mixed SAMs. The results suggest that in all cases the ET rates are modulated by low-amplitude motions of the protein and thermal fluctuations of interfacial water molecules, which in turn are influenced by the interfacial electric field.

2. Results and Discussion

2.1. Structural and Redox Equilibria of the Immobilized Protein

Nanostructured Ag electrodes were coated with SAMs of different compositions for subsequent immobilization of horse heart Cyt-c. The different films include single-component SAMs of 6-mercaptohexanoic acid (C5-COOH) and of 11-mercaptoundecanoic acid (C10-COOH), as well as mixed SAMs of 1:1 mixtures of C5-COOH/6-mercaptohexan-1-ol (C5-COOH/C6-OH) and of C10-COOH/11-mercaptoundecan-1-ol (C10-COOH/C11-OH). All experiments were carried out at pH 7.0 such that the SAMs ex-

hibited a negatively charged surface due to partial dissociation of the carboxylic acid tail groups, thereby allowing the positively charged Cyt-c to bind electrostatically, as reflected by the strong and characteristic SERR signals. The SERR spectra of ferrous Cyt-c adsorbed on the different SAMs, recorded upon Soret-band excitation, are identical to the corresponding resonance Raman (RR) spectrum in solution, that is, the structure of the heme pocket is preserved upon adsorption. Furthermore, the sensitive response of the spectra to the applied electrode potential indicates that Cyt-c undergoes direct electrochemistry in all of the SAM/Cyt-c electrostatic complexes investigated, in agreement with previous findings.[2,3] Within the potential range from −400 mV to about 50 mV (vs. Ag/AgCl), all SERR spectra can be quantitatively described by a superposition of the RR spectra of the native state of Cyt-c (denoted as state B1), with variable contributions of the reduced and oxidized forms (Figure 1). The relative contributions of the component spectra of reduced and oxidized forms obtained in this way were converted to relative surface concentrations by using proportionality factors determined by RR spectroscopy of the pure species in solution.[43] The resultant potential-dependent changes of the relative concentrations were then analyzed in terms of the Nernst equation for determining the standard reduction potentials E°. As summarized in Table 1, Cyt-c electrostatically adsorbed to the different SAMs exhibits nearly ideal Nernst behavior with E° values slightly more negative than determined for Cyt-c in solution. These negative shifts can be ascribed to the potential drop across the SAMs.[40]

The SERR spectra recorded at very negative potentials reveal a small contribution (<5%) of native but redox-inactive species which are attributed to proteins immobilized with orientations of very weak electronic coupling (Figure 2).[27,39] For electrode potentials above 50 mV, the component analysis of the SERR spectra reveals small contributions of the so-called B2 species of Cyt-c (Figure 2), in which the Met-80 axial ligand is removed from the heme iron atom to give five-coordinate high-spin heme species. This species is in equilibrium with a non-native six-coordinate low-spin form in which the Met-80 ligand is replaced by a His residue.[3,40] This structural transition to the B2 state is only observed for the ferric protein, whereas upon reduction the B1 form is recovered.

Cyt-c was covalently attached to the various SAMs described above by using two different cross-linking reagents and procedures (A and B; see Experimental Section) that are expected to yield differently oriented samples. In both cases the final step consists of removal of the residual physisorbed Cyt-c by thorough washing with buffered KCl solutions. The desorption procedure was optimized by monitoring the SERR signal as a function of time after dipping the Cyt-c-loaded electrodes into KCl solutions of different concentrations (Figure 3). Accordingly, immersion of the electrodes in 2 M KCl solution for 15 min, followed by gentle rinsing with the buffer solution, was found to remove 95% of the physisorbed species from the electrode surface. This protocol was applied to the electrode loaded with Cyt-c immobilized by covalent cross-linking such that the contribution of electrostatically bound Cyt-c to the resultant SERR spectra was always negligibly small. Treatment with a sulfate-containing solution of the same ionic strength did not cause complete desorption of the physisorbed proteins.

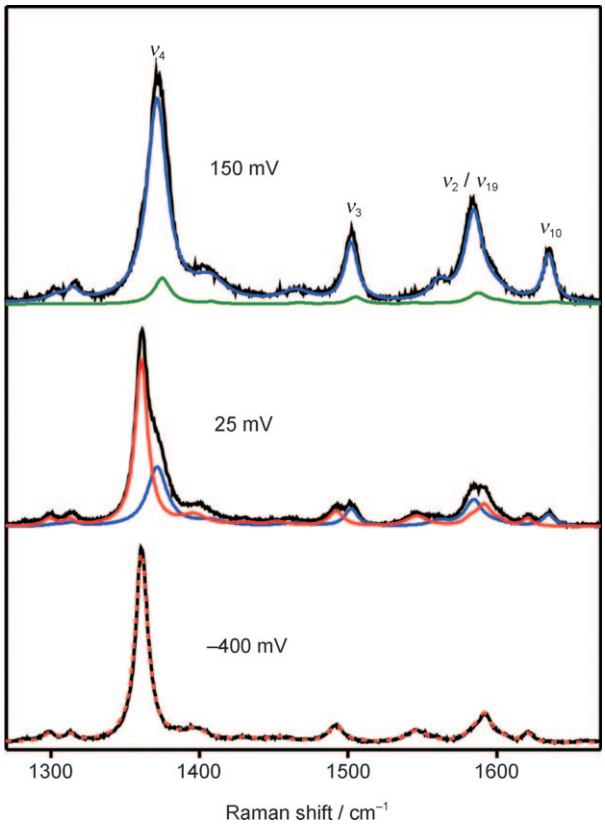

Figure 1. Soret-band SERR spectra measured at various potentials for Cyt-c electrostatically adsorbed on a Ag electrode coated with a 1:1 C10-COOH/C11-OH SAM. The experimental spectra are given by the black lines, whereas the component spectra of the oxidized B1, the reduced B1, and the oxidized B2 states are represented by the blue, red, and green lines, respectively.

Table 1. Thermodynamic and kinetic parameters obtained by SERR for Cyt-c in electrostatic and covalent complexes with different SAMs. Kinetic constants for C10 and C5 SAMs refer to potential jumps from 41 to −200 mV and from 50 to −50 mV, respectively.

SAM	Electrostatic binding				Covalent binding[a]			
	C5-X		C10-X		C5-X		C10-X	
tail group (X)	CO_2H	CO_2H/CH_2OH	CO_2H	CO_2H/CH_2OH	CO_2H	CO_2H/CH_2OH	CO_2H	CO_2H/CH_2OH
E^0 [mV]	15±5	19±3	20±2	21±2	6±5	21±5	3±5	18±4
n	0.8	0.9	0.9	0.9	0.6	0.5	0.6	0.5
k_{redox} [s^{-1}][b]	220±20	113±10	160±20	170±20	120±25	125±10	125±30	120±20
$^bk_{orient}$ [s^{-1}][c]	250±25	170±40	400±100	250±50	n.d.[d]	n.d.[d]	n.d.[d]	n.d.[d]

[a] Covalent complexes prepared according to procedure A. [b] Determined by TRSERR with Soret-band excitation. [c] Determined by TRSERR with Q-band excitation; [d] n.d. = not determined

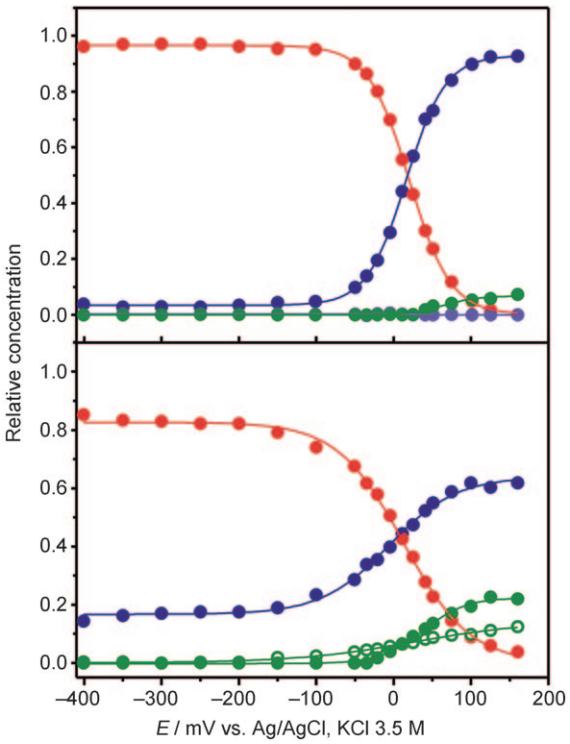

Figure 2. Relative concentrations of the different states of Cyt-c electrostatically (top) and covalently bound (bottom) to C10-COOH/C11-OH SAMs, as determined from Soret-band SERR spectra recorded as a function of the applied potential. The solid blue, red, green, and the open green symbols refer to the oxidized B1, the reduced B1, the oxidized B2(6cLS), and the oxidized B2(5cHS) states, respectively.

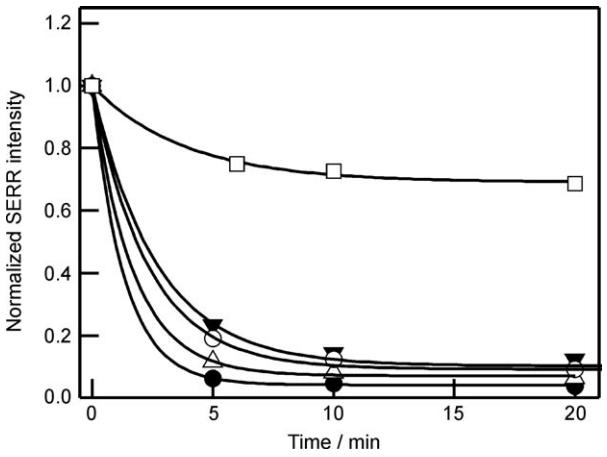

Figure 3. Normalized SERR intensities of the ν_4 band of reduced Cyt-c (B1) as a function of the time of immersion in KCl solution of different concentrations after immobilization by procedure A. Concentrations of KCl: 0.2 M (open squares), 1.0 M (filled black triangles), 2.0 M (open circles), 3.0 M (open triangles), saturated solution (filled black circles).

Potential-dependent SERR spectra of Cyt-c covalently attached to the various SAMs were measured in the potential range from −400 to 50 mV, and their analysis in terms of different contributions of the ferric and ferrous forms of state B1 indicated that the chemical immobilization procedure does not affect the structure of the redox center. However, about 10–15% of the bound protein could not be reduced even at the most negative potentials used (Figure 2). We ascribe this observation to the nonspecificity of the coupling reaction, which in principle can lead to Cyt-c binding through any of the 11 lysine residues on the protein surface, so that a subpopulation of protein molecules that are not able to establish efficient electron pathways to the electrode results. Accordingly, Nernst plots of covalently attached Cyt-c deviate from ideality with a number of transferred electrons of 0.5–0.6 and slightly more negative reduction potentials than observed for electrostatic adsorption (Table 1 and Figure 2). As in the case of electrostatic adsorption, SERR spectra indicate the formation of small amounts of B2 species for potentials above 50 mV.

2.2. Orientation of the Immobilized Protein

For symmetric molecules, the surface-enhanced Raman (SER) spectrum includes information about the orientation with respect to the surface,[44] because for modes of different symmetry the individual components of the scattering tensor are modified to different extents depending on their relative orientation with respect to the electric field vector. As a consequence, vibrational modes of different symmetry may experience different enhancements. In the specific case of the heme group which, in a first approximation, has D_{4h} symmetry, it can be shown that the totally symmetric A_{1g} modes will experience preferential enhancement when the heme plane is parallel to the surface, while for a perpendicular orientation the A_{1g} modes as well as the nontotally symmetric A_{2g}, B_{1g}, and B_{2g} modes will be enhanced to the same extent.[30] Therefore, different orientations of the adsorbed heme protein are expected to lead to different intensity ratios of modes of different symmetries, for example, $\nu_{10}(B_{1g})/\nu_4(A_{1g})$. This is strictly true only under nonresonant excitation conditions which, however, would imply the loss of selectivity in probing the cofactor spectrum. A reasonable compromise between an acceptable molecular resonance enhancement and qualitatively predictable selection rules may be achieved upon excitation close to the weak Q bands of the heme group. This approach was previously used to monitor orientational changes of Cyt-c electrostatically adsorbed on electrodes coated with single-component SAMs of ω-carboxyl alkanethiols.[27,30] In that work, it was shown that the orientation of the protein in the SAM/Cyt-c electrostatic complexes is dependent on the electric field and thus varies with the chain length of the ω-carboxyl alkanethiol and the applied electrode potential. Use of this method in the present study indicated that dilution of the carboxyl-terminated thiols by addition of ω-hydroxyl alkanethiols does not have a significant impact on the average orientation of Cyt-c electrostatically adsorbed on the SAMs. Both the absolute $\nu_{10}(B_{1g})/\nu_4(A_{1g})$ ratios and their dependence on potential are very similar to those of the pure carboxyl-terminated SAMs (Figure 4). Similar to single-component SAMs,[27,30] the $\nu_{10}(B_{1g})/\nu_4(A_{1g})$ ratios decrease for the longer SAMs, which is consistent with the proposed electric-field dependence of the orientation and indicates a more perpendicular average orientation of the

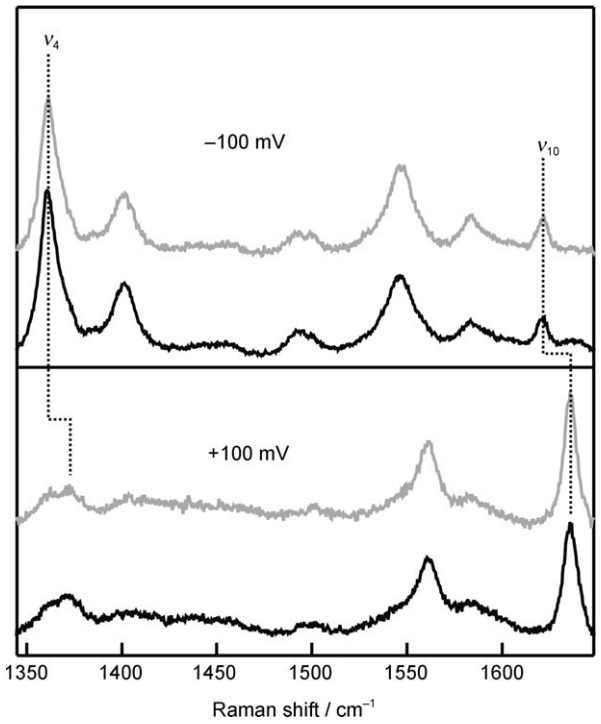

Figure 4. Q-band SERR spectra of Cyt-c in electrostatic complexes with C5-COOH (black) and C5-COOH/C6-OH (gray) SAMs recorded at −0.1 (top) and +0.1 V (bottom).

heme group with respect to the electrode surface for shorter SAMs, that is, at higher electric fields.

Upon covalent binding of the protein to the SAMs by using cross-linking procedure A, the $\nu_{10}(B_{1g})/\nu_4(A_{1g})$ intensity ratio drops with respect to the corresponding electrostatic complexes by factors of about 2 and 1.3 for the shorter and longer SAMs, respectively. These results indicate that, in the covalent complexes, ferric Cyt-c is oriented with the heme group less perpendicular to the surface than upon electrostatic binding. At first sight, a different average orientation of the electrostatically bound and the covalently attached Cyt-c may be surprising, since protocol A for covalent cross-linking is based on electrostatic pre-adsorption of the protein to the SAM. However, the lysine residues directly interacting with the carboxyl functions of the SAM are less accessible for the cross-linker EDC, such that amide bond formation may be favored for adjacent lysine residues. Furthermore, these steric constraints may lead to a less homogeneous average orientation of the covalently bound Cyt-c, which is consistent with the broad redox transitions (see above). It appears that covalent attachment according to procedure A lowers the stability of the protein. When the electrode potential is set to $E > E^0$, slow and partially irreversible transition to the B2 or a B2-like state is observed with time constants on the order of seconds or minutes even for thick C11-SAMs (see Supporting Information, Figure S1). Such a transition has not been noted for Cyt-c electrostatically bound to SAMs of the same thickness. Covalent attachment of Cyt-c by procedure A does not inhibit reorientation of the protein, as demonstrated by the dependence of the $\nu_{10}(B_{1g})/\nu_4(A_{1g})$ intensity ratio on potential, although the variation with potential is weaker than for electrostatically bound Cyt-c (Figure 5). The situation is different when Cyt-c is covalently attached by cross-linking procedure B. Here, the average orientation of the heme group with respect to the electrode surface appears to be even less perpendicular and, in contrast to covalent immobilization by procedure A, it is independent of the applied potential (Figure 5).

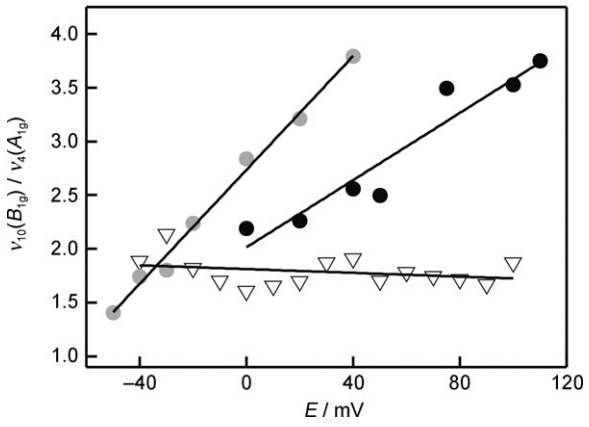

Figure 5. Potential dependence of the $\nu_{10}(B_{1g})/\nu_4(A_{1g})$ intensity ratio as determined by Q-band SERR for oxidized Cyt-c immobilized on C10-COOH SAMs by different strategies. Gray filled circles: electrostatic adsorption; black filled circles: cross-linking procedure A; empty triangles: cross-linking procedure B.

2.3. Electron Transfer and Orientation Dynamics

It is well established that the heterogeneous ET rate constant of Cyt-c in electrostatic complexes with SAMs of long chain ω-carboxy alkanethiols exhibits the exponential dependence on distance characteristic of the tunneling mechanism, but it levels off when the number of methylene groups of the thiol is reduced to less than ten.[2,3,23,31–36] This behavior is confirmed by the present TRSERR experiments on electrostatically bound Cyt-c carried out with an overpotential of −100 mV (Figure 6).

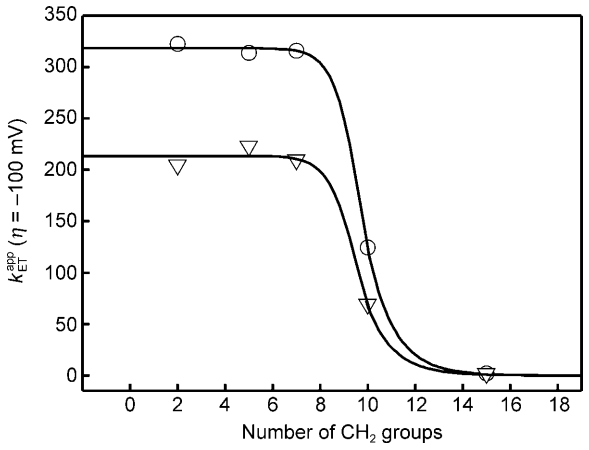

Figure 6. Distance dependence of the apparent ET rate constants k_{ET}^{app} of Cyt-c immobilized on C11-COOH SAMs, as determined by TRSERR spectroscopy for overpotentials of −100 mV. Empty circles: electrostatically adsorbed protein; empty triangles: protein cross-linked by procedure B.

The spectral analysis did not provide any indication for involvement of species other than the reduced and oxidized form B1 in the interfacial redox process.[3,40,43] Essentially the same kinetic behavior is observed when the protein is electrostatically adsorbed on mixed C10-COOH/C11-OH SAMs; the TRSERR experiments yield very similar results (Table 1), in line with previous findings by Davis et al.[42] For the shorter SAMs, however, we observe a drop of the apparent ET rate by a factor of two when comparing C5-COOH with C5-COOH/C6-OH (Table 1). Q-band-excited TRSERR spectra of electrostatically bound Cyt-c reveal that, regardless of the SAM composition, thinner films yield reorientation rates that are nearly identical to the ET rates obtained from TRSERR experiments with Soret-band excitation. These results are consistent with a gated mechanism, as recently proposed for single-component SAMs,[2,27,30] in which the overall redox process is controlled by the electron-tunneling probability at long distances, but protein reorientation becomes rate-limiting for the thinner films.

Covalent binding of Cyt-c to single-component or mixed SAMs by cross-linking procedure A has a relatively small effect on k_{ET}^{app} compared to the analogous electrostatic complexes (Table 1), except for C_5-COOH SAMs, for which a value nearly two times smaller is determined. The overall similar kinetic behavior suggests that also for the covalent Cyt-c-SAM complexes prepared according to procedure A the same gated mechanism holds, even though the kinetics of the reorientation process could not be determined in an equally reliable manner, mainly due to the smaller potential-dependent changes of the $\nu_{10}(B_{1g})/\nu_4(A_{1g})$ intensity ratio compared to the electrostatic complexes (Figure 5). In this respect, the results obtained for the covalently bound Cyt-c obtained by procedure B are quite unexpected. Despite the lack of any detectable potential-dependent orientational changes, reflected by the essentially constant $\nu_{10}(B_{1g})/\nu_4(A_{1g})$ intensity ratio (Figure 5), the k_{ET}^{app} values determined from the TRSERR experiments display qualitatively the same distance dependence as the electrostatically adsorbed protein (Figure 6), albeit with generally lower k_{ET}^{app} values. Also the overpotential dependence of k_{ET}^{app} for C10-COOH SAMs is qualitatively similar to that the electrostatic complexes (Figure 7), again with a limiting value that is ca. 30% lower. When the relative viscosity of the solution is increased to 1.5 cP by addition of sucrose, the k_{ET}^{app} values show a decrease at the higher overpotentials which is more severe than for the covalent complex obtained by procedure A. A fit of Equation (2) to the experimental data for the overpotential dependence of k_{ET}^{app} affords an apparent reorganization energy of $\lambda_{app} = 0.23$ eV for Cyt-c electrostatically adsorbed to C10-COOH SAMs. This value is in good agreement with that previously determined for Cyt-c at C15-COOH, for which electron tunneling is the rate limiting step. This finding is consistent with the fact that the reorientation rate is almost independent of the applied overpotential (within the applied range) and that k_{reor}^{app} is larger than the limiting value of k_{ET}^{app} (Figure 7). A 50% increase in solution viscosity causes a drop of the reorientation rate of the electrostatically adsorbed protein that results in a slight decrease of the k_{ET}^{app} values at the higher overpotentials. As a consequence a slightly lower value of 0.19 eV is determined for λ_{app}. For the protein covalently bound by following procedure B, the overpotential dependence of k_{ET}^{app} yields $\lambda_{app} = 0.20$ eV at $\rho = 1$ cP, that is, a lower value than for the electrostatic complex at 1 cP and very close to the value obtained at 1.5 cP.

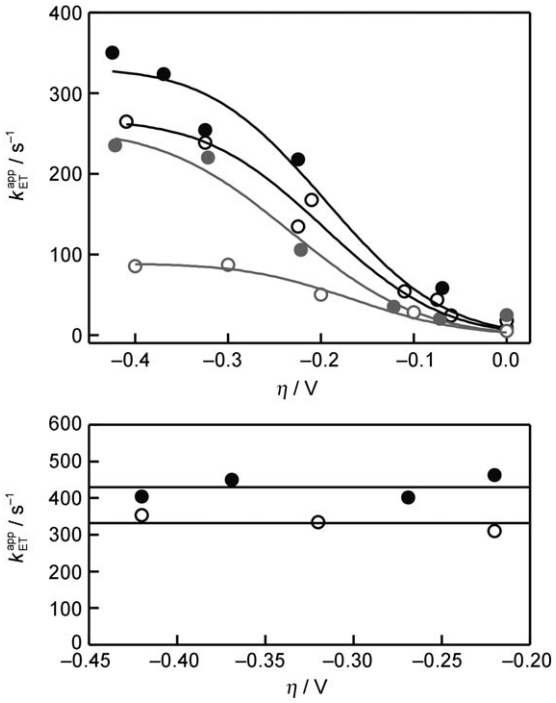

Figure 7. Top: Overpotential dependence of k_{ET}^{app} for Cyt-c immobilized on C10-COOH SAMs in normal phosphate buffer ($\rho = 1$ cP; filled symbols) and phosphate buffer with addition of sucrose ($\rho = 1.5$ cP; empty symbols). Black circles: electrostatically adsorbed protein; gray circles protein cross-linked by method B. Bottom: Overpotential dependence of k_{reor}^{app} for C10-COOH/Cyt-c electrostatic complexes at 1 cP (filled circles) and 1.5 cP (open circles).

2.4. Molecular Dynamics Simulations

In previous computational work we studied the adsorption, dynamics, and electronic coupling of Cyt-c on metal surfaces coated with SAMs of ω-carboxyl alkanethiols.[27,39] It was shown that the protein exhibits three main binding domains of different affinity. Binding through any of the domains does not lead to rigid electrostatic complexes, and instead the protein exhibits significant mobility that modulates the electronic coupling. The simulations predict that small-amplitude motions of the protein may have a substantial effect on the heterogeneous ET rate. For instance, changes of the tilt angle of the heme plane with respect to the electrode surface as small as 5° may result in a variation of the electronic coupling of one order of magnitude, corresponding to variations of k_{ET} by two orders of magnitude. Furthermore, large-amplitude rotations of the protein on the SAM surface are strongly suggested, although they cannot be captured within the timescale of the simulations. Such rotations have a direct impact on the order of magnitude of the electronic coupling, while fine tuning is exerted by

structural thermal fluctuations of the proteins and solvent molecules.[27,39]

Herein, we applied the same methodology for investigating the ET properties of Cyt-c covalently bound to similar SAMs. For the in silico covalent linkage we selected as representative examples four different lysine residues: lysines 79 and 86, which are included in the main binding domains MZI and MZII of the ferric protein, and lysines 13 and 72, which are included in MZI and MZII of ferrous Cyt-c.[27,39] Single amide bonds with the SAM were formed in each case. For all binding configurations, MD simulations were run in explicit water environment for 10 ns and optimal electronic couplings V^{max} were computed every 10 ps by using the pathway algorithm. Figure 8 shows the mobility of the protein in terms of the angles α and ϕ that describe the orientation of the heme group with respect to the metal surface (see Experimental Section for definition of α and ϕ and further computational details). The high-frequency mobility of the covalently attached protein is very similar to that observed for electrostatic adsorption through the same region, and thus leads to comparable fluctuations of the electronic coupling along the simulation. Similarities and differences can be better appreciated in the histograms shown in Figure 9. For the angle α, the electrostatic and covalent complexes have almost identical distributions centered at 112°, while for ϕ the covalent complex is slightly shifted to lower values (maxima at 170 and 172°, respectively). Note that the dynamics of Cyt-c in electrostatic and covalent complexes shown in Figure 8 are rather similar during the first 8 ns. At this point in time the electrostatically adsorbed protein rotates by 10 and 20° in α and ϕ directions, respectively, which is also evident as a shoulder in Figure 9. The resulting orientation exhibits a lower average coupling, and no large amplitude peaks are detected for the remaining 2 ns. As a consequence, the ET rate in this orientation is expected to be significantly lower. This large-amplitude rotation is impeded in the covalent complex. Similar results were obtained for all cases studied.

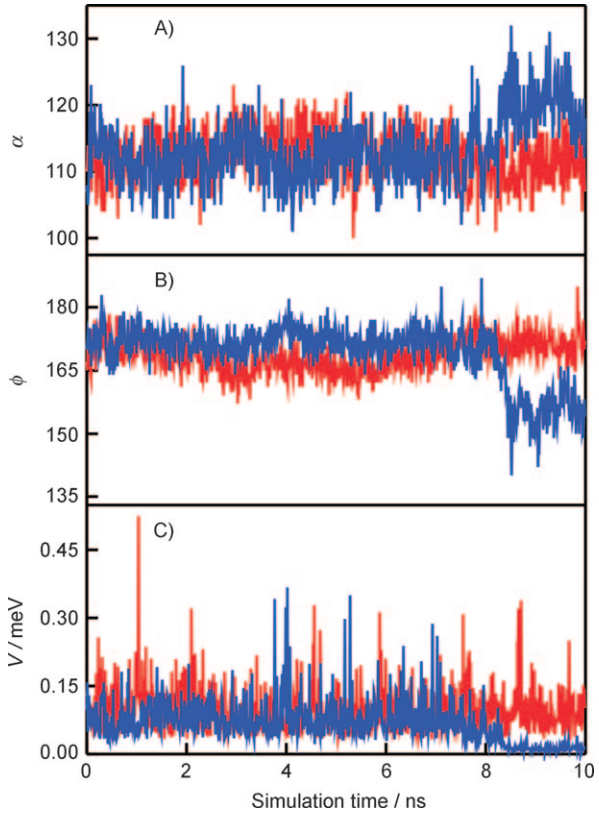

Figure 8. Variation of α (A), ϕ (B), and V (C) as a function of simulation time for oxidized Cyt-c cross-linked to a SAM through Lys86 (red) compared with the variations of the same parameters for the equivalent electrostatic complex (blue).

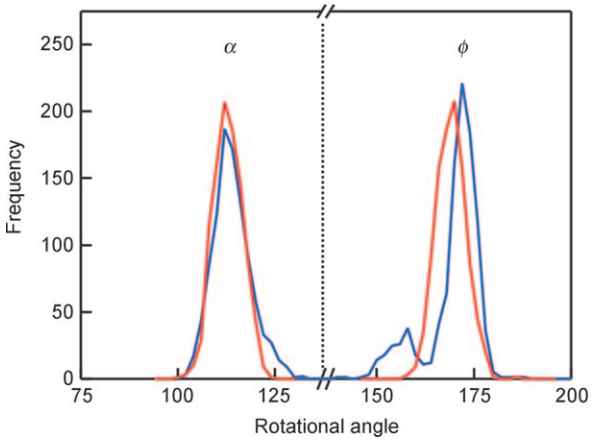

Figure 9. Histograms of the angles α and ϕ determined along the 10 ns simulations for electrostatic (blue) and covalent (red) SAM/Cyt-c complexes.

A summary of the results obtained for the different binding configurations and redox states is presented in Table 2. In all cases the adsorbed and covalently attached proteins exhibit

Table 2. Average values of α, ϕ, and V, maximum coupling V^{MAX} and optimal electron pathways obtained for the different immobilization modes of Cyt-c, as obtained by MD simulations.

Redox state	Binding site	$<\alpha>$	$<\phi>$	$\langle V\rangle$ [meV]	V^{MAX} [meV]	ET path[a]
Covalent binding						
Fe^{2+}	Lys13	93.8	172	0.14 ± 0.075	0.61	Hec–Cys–SAM
	Lys72	96	186	0.72 ± 0.36	2.18	Hec–Cys–SAM
Fe^{3+}	Lys79	112	168	0.095 ± 0.046	0.52	Hec–Vinyl–SAM
	Lys86	101	193	0.31 ± 0.12	0.88	Hec–Vinyl–SAM
Electrostatic binding						
Fe^{2+}	MZI (Lys13)	87	183	0.44 ± 0.20	1.44	Hec-Cys-SAM
	MZII (Lys72)	92	185	0.50 ± 0.25	1.71	Hec–Cys–SAM
Fe^{3+}	MZI (Lys79)	113	171	0.067 ± 0.045	0.36	Hec–Wat–SAM
	MZII (Lys86)	105	195	0.41 ± 0.20	1.74	Hec–Methyl–SAM

[a] Hec: heme tetrapyrrole ring, Cys: cysteine 17, Methyl: methyl substituent of ring D, Wat: water molecule.

comparable average and maximum couplings as well as standard deviations.

2.5. Interplay of Electron Transfer and Protein Dynamics

The TRSERR results presented here show that the distance dependence of the heterogeneous ET rate of Cyt-c on SAM-coated electrodes follows qualitatively the same tendency whether the protein is electrostatically adsorbed or cross-linked to the SAMs. The kinetic behavior includes the characteristic exponential variation for long SAMs and little or no variation for the shorter ones. In quantitative terms, however, k_{ET}^{app} for the covalently attached protein is lower in the plateau region. In all cases, k_{ET}^{app}, measured for short SAMs or high driving forces, drops upon increasing the viscosity of the solution in contact with the immobilized protein, and this suggests that under these conditions the rate-limiting event is related to protein motion. Stationary SERR experiments performed under Q-band excitation show a distinct potential dependence of the average protein orientation for electrostatically bound Cyt-c and for covalent SAM/Cyt-c complexes prepared according to procedure A, although in that case the variation is smaller. At first sight this result is surprising, since formation of the amide bond between the protein and the SAM is expected to restrict the mobility. Although this is true for large-amplitude motion, MD simulations show that the low-amplitude mobility (thermal fluctuations) in the complexes formed through electrostatic interactions and through equivalent single covalent bonds are rather similar and, furthermore, that these subtle fluctuations are sufficient for producing significant changes of the tunneling probabilities. Thus, the present experimental results for the covalently bound Cyt-c prepared according to procedure A are consistent with formation of a single amide bond that allows for a similar orientation and low-amplitude mobility as in the electrostatic complex. Small populations of differently oriented protein or multibond formation cannot be discarded and, in fact, are strongly suggested by the less ideal electrochemical response and the slightly lower variation of the $\nu_{10}(B_{1g})/\nu_4(A_{1g})$ ratio with the potential in comparison with the electrostatic complex. For electrostatically bound Cyt-c the transition from the tunneling-controlled to the orientation-controlled ET regime has been proposed to be governed by the increasing interfacial electric field with decreasing SAM length, which slows down the mobility of the protein. The experimentally determined rate of reorientation of Cyt-c in electrostatic complexes with C5-COOH SAMs is about two orders of magnitude slower than that for C15-COOH SAMs,[30] corresponding to an approximately twofold increase of the interfacial electric field.[45] In agreement with this interpretation, MD simulations on similar SAM/Cyt-c electrostatic complexes suggest that the rate of reorientation from the high-affinity domain with low electronic coupling configuration to the optimal orientation for ET decreases by more than one order of magnitude in the presence of an electric field strength of 0.01 V Å^{-1} and more than 11 orders of magnitude when the field strength is 0.1 V Å^{-1}.[39] In view of the quite similar overall kinetic behavior compared to electrostatically bound Cyt-c, we conclude that, also for the covalent Cyt-c/SAM complex obtained by procedure A, the local electric field strength determines the protein mobility, despite partial neutralization of surface charges by the cross-linking procedure.

According to the MD calculations, one would further expect that, at sufficiently high fields, k_{ET}^{app} should decrease after reaching a maximum. This behavior has not been observed for SAMs of ω-carboxyl alkanethiols, evidently because even for the shortest possible chain length with only one methylene group, the electric field is not sufficiently strong. A decrease of k_{ET}^{app}, however, has in fact been observed upon replacing the carboxyl group by divalent anions to increase the charge density at the interface and thus the electric field for the electrostatically bound Cyt-c.[3] The distance dependence of k_{ET}^{app} for Cyt-c covalently bound according to procedure B is qualitatively similar to the two modes of protein immobilization discussed above (electrostatic and covalent through procedure A), including the viscosity sensitivity in the plateau region. However, SERR experiments performed with Q-band excitation do not show any appreciable variation of the $\nu_{10}(B_{1g})/\nu_4(A_{1g})$ ratio with potential. This striking discrepancy indicates that procedures A and B lead to different covalent Cyt-c/SAM complexes. According to protocol A, cross-linking is carried out with the electrostatic ferrous Cyt-c/SAM complex formed at a negative potential, while in protocol B the SAM is activated prior to coupling of ferric Cyt-c at open circuit. Thus, procedures A and B yield slightly different distributions of orientations, as reflected by the different $\nu_{10}(B_{1g})/\nu_4(A_{1g})$ intensity ratios. In addition, protocol B includes the addition of NHS and significantly longer incubation times, and thus is expected to afford higher protein coverage, as indicated by the stronger SERR signals. On the other hand, albeit not verified experimentally, it is reasonable to assume that protocol B should lead to the formation of more than one amide bond per Cyt-c molecule.[42] If this were the case the covalently attached protein would exhibit a much more restricted mobility consistent with a potential-independent $\nu_{10}(B_{1g})/\nu_4(A_{1g})$ intensity ratio. However, low-amplitude motions that refers to thermal fluctuations of the protein and interfacial solvent molecules are not inhibited and may result in a distinct modulation of the optimum electron pathways and thus of the ET rate.[27,39] Moreover, depending on the positions of the amide bonds the mobility of the protein can be restricted with respect to the angle α, ϕ, or both. If the protein were attached through two bonds that are contained in a plane perpendicular to the heme group, then rotation with respect to α, but not to ϕ, would be largely restricted. As a consequence, SERR experiments would reveal no changes of the $\nu_{10}(B_{1g})/\nu_4(A_{1g})$ intensity ratio that are only sensitive to variation of α. Conversely, thermal fluctuations and low-amplitude rotations with respect to ϕ that are not detectable in SERR experiments may still occur and modulate the electronic coupling. Then, as in the previous cases, protein dynamics is expected to be rate-limiting for thin SAMs, that is, at high electric fields, as suggested by the large viscosity effects observed for short SAMs or high driving forces.

Consistent with this interpretation are previous findings by Jin et al., who showed that, in contrast to electrostatically im-

mobilized Cyt-c, the covalently bound protein prepared according to procedure A is not capable of shuttling electrons between the electrode and NADPH cytochrome P450 reductase in the solution phase.[46] Here a major reorientation is required to switch between electron exchange with the electrode and the reductase, a movement of Cyt-c that is blocked upon covalent attachment already under "mild" conditions.

Conclusions

The results presented here show that the experimentally determined rate constants for the heterogeneous ET of Cyt-c immobilized on SAM-coated electrodes represent a convolution of orientation-dependent tunneling probabilities and the orientational distribution and dynamics of the protein ensemble. In electrostatic complexes with negatively charged SAMs, the relatively narrow orientational distribution leaves the vast majority of molecules in an orientation that is not optimized for ET. A qualitatively similar conclusion is reached for the protein cross-linked to these SAMs, although in this case the distribution of orientations is broader and the mobility is restricted specifically when the protein is attached by more than one covalent amide bond. However, even in the covalent complexes, low-amplitude motions of the proteins and interfacial water molecules guarantee transient pathways of sufficiently high electronic coupling. For thick SAMs, electron tunneling is significantly slower than protein and solvent dynamics, and thus the measured rates represent a true ET rate that exhibits the characteristic exponential dependence on distance. For thinner SAMs, that is, higher charge densities and stronger electric fields, protein and solvent dynamics is significantly slowed down and becomes rate-limiting. This kinetic behavior is likely to be rather general and may constitute the basis for the unusual distance dependencies of the ET rates reported for a variety of redox proteins in electrochemical studies.[21–26] A similar mechanism is likely to operate when Cyt-c exerts its electron-transport function in aerobic respiration. As suggested by various studies, the initial electrostatic complex of Cyt-c with the natural reaction partner Cyt-c oxidase is not optimized for ET and thus requires reorientation.[47] According to the results presented here, such reorientation processes can be expected to be modulated by the variable transmembrane potential, which thus would play a role in inhibitory control of the ET-driven proton translocation activity.

Experimental Section

Chemicals: 6-Mercaptohexanoic acid (C5-COOH) was purchased from Dojindo. All other chemicals, including 11-mercaptoundecanoic acid (C10-COOH), 11-mercaptoundecan-1-ol (C11-OH), 6-mercaptohexan-1-ol (C6-OH), *N*-ethyl-*N*′-(3-dimethylaminopropyl) carbodiimide (EDC), *N*-cyclohexyl-*N*′-(2-morpholinoethyl)carbodiimide methyl-*p*-toluenesulfonate (CMC), and *N*-hydroxysuccinimide (NHS), were purchased from Sigma-Aldrich and used without further purification. Horse heart cytochrome c (Cyt-c) was purchased from Sigma-Aldrich and purified by HPLC. The water used in all experiments was purified by a Millipore system and its resistance was greater than 18 MΩ.

Electrode Modification: Silver ring electrodes were mechanically polished with 3M polishing films from 30 to 1 μm grade. After washing, electrodes were subjected to oxidation–reduction cycles in 0.1 M KCl to create an SER-active nanostructured surface. Subsequently, the electrodes were incubated in 1.5 mM ethanolic solutions of the alkanethiols (pure or 1:1 mixtures) for ca. 20 h, and then rinsed and transferred to the spectroelectrochemical cell. For electrostatic adsorption Cyt-c was added to the electrochemical cell from a stock solution to form a 0.2–0.4 μM solution and allowed to incubate at room temperature for ca. 15–20 min before starting the experiments.

Covalent Binding: Two different procedures were used for cross-linking of Cyt-c to the SAMs. In procedure A, the protein was adsorbed on the SAM-coated working electrode for about 20 min. at −100 mV as in the case of electrostatic binding. Subsequently, EDC was added to the cell from a stock solution to obtain a 5 mM concentration. The resulting solution was stirred for 45 min while maintaining the applied potential (−100 mV). The electrode was then rinsed with water and exposed to a 2–3 M KCl solution for 15 min at open circuit to remove remaining electrostatically adsorbed protein.

In procedure B, The SAM-coated electrodes were incubated for 2 h in a de-aerated solution of CMC (20 mg/10 mL) and NHS (6 mg/10 mL). After activation of the carboxyl groups, the electrode was rinsed thoroughly and immersed in a 10 mM Cyt-c solution containing 30 mM phosphate buffer solution (pH 7) overnight. Finally, the electrode was thoroughly rinsed with water and then immersed in a 2–3 M KCl solution for 10 min to desorb the remaining physisorbed protein. In contrast to procedure A, all steps were performed at open circuit.

Surface-Enhanced Resonance Raman Spectroscopy: The spectroelectrochemical cell for SERR spectrosocpy has been described elsewhere.[40] Briefly, a Pt wire and a Ag/AgCl electrode were used as counter- and reference electrodes, respectively. All potentials cited in this work refer to the Ag/AgCl (3 M KCl) electrode. The working electrode was a silver ring of 8 mm diameter and 2.5 mm height mounted on a shaft that is rotated at about 5 Hz to avoid laser-induced sample degradation.

The electrolyte solution (30 mM phosphate buffer, pH 7.0) was bubbled with catalytically purified oxygen-free argon prior to the measurements, and Ar overpressure was maintained throughout the experiments. The viscosity of the solution was adjusted by addition of sucrose to the same buffer, which has been shown not to affect significantly the dielectric constant.[33]

SERR spectra were measured in backscattering geometry by using a confocal microscope coupled to a single-stage spectrograph (Jobin Yvon, LabRam 800 HR or XY 800) equipped with a liquid-nitrogen-cooled back-illuminated CCD detector. Elastic scattering was rejected with notch or edge filters. The 413 nm line of a cw krypton ion laser (Coherent Innova 300c) or the 514 nm line of a cw argon laser (Coherent Innova 70c) was focused onto the surface of the rotating Ag electrode by means of a long-working-distance objective (20×, N.A. 0.35). Typically, experiments were performed with laser powers of about 1 mW (413 nm) and 5–12 mW (514 nm) at the sample. Effective acquisition times were between 3 and 10 s. All experiments were repeated several times to ensure reproducibility.

For TRSERR experiments, potential jumps of variable height and duration were applied to trigger the reaction. The SERR spectra were measured at different delay times following the potential

jump. Synchronization of potential jumps and probe laser pulses was achieved by a pulse-delay generator (BNC). The probe pulses were generated by passing the cw laser beam through two consecutive laser intensity modulators (Linos), which give a total extinction better than 1:50 000 and a time response of ca. 20 ns. Details of the TRSERR measurements are described elsewhere.[23,30]

After background subtraction the spectra were treated by single-band (514 nm) or component analysis[43] (413 nm) in which the spectra of the individual species were fitted to the measured spectra by using a home-made analysis software. The time-dependent changes of the relative concentrations of the species involved were subsequently analyzed in terms of relaxation kinetics to yield reciprocal relaxation time constants.[24]

Molecular Dynamics Simulations: The computational methods for comparing the covalent and electrostatic SAM/Cyt-c complexes have been presented and discussed previously,[27,39] and therefore they will be only briefly described here.

Initial Cyt-c structures were obtained from the PDB database (PDB 26IW and PDB 1HRC for the reduced and oxidized form, respectively). For simulating the SAMs, an infinite array of fixed Au atoms with lattice structure 111 was built in silico, and each of them was linked to a C5-COOH molecule through the S atom. SAM and lattice parameters were adopted from the literature.[27,39] The infinite array consisted of a periodic boundary condition (PBC) cell of 13×14 Au atoms in the *X* and *Y* directions, with their corresponding alkanethiols. In the *Z* direction periodicity is achieved by using periodic boxes of 80 Å width, which leaves sufficient space between the Cyt-c surface and the next (upper) gold layer to avoid direct interaction. Cross-linking of Cyt-c to the SAMs was performed by in silico modification of selected protein Lys residues and SAM carboxylate groups to an amide bond.

The production simulations of each complex were performed by immersing the SAM/Cyt-c structures contained in a TIP3P water box. For each case, an initial constant-volume MD was performed to heat the system to 300 K, and subsequently a constant-pressure simulation was performed to equilibrate the system density. Finally, production MDs were performed. Temperature and pressure were kept constant using the Berendsen thermostat and barostat. For the PBC simulations, Ewald summations were employed to compute the electrostatic energy terms by using the default parameters in the Sander module of the AMBER package.

The orientation of Cyt-c with respect to the Au/SAM surface was defined based on the relative heme orientation in terms of two angles: the angle α between the Fe–S(Met80) bond, which is perpendicular to the heme plane, and the *Z* axis of the system, which is perpendicular to the Au/SAM surface. Values of α close to 0 or 180° imply that the heme group lies parallel to the SAM, whereas a value of 90° corresponds to perpendicular orientation of the heme plane with respect to the surface. The angle ϕ is determined by the vector defining the Fe–N_A bond (where N_A is the nitrogen atom of the pyrrolic ring) and the vector pointing towards the SAM, which lies in the heme plane. This angle describes the rotational orientation of the heme group and thus of the entire Cyt-c. Values between 0 and 90° correspond to protein orientations in which the heme propionate groups are closer to the SAM surface, whereas for values between 180 and 270° the propionate groups point away from the SAM surface. Note that for α values close to 0 or to 180° changes of the ϕ value do not correspond to significant variations of protein orientation since the heme group lies parallel to the SAM surface.

Coupling Matrix calculation: The electronic coupling between the heme iron atom and any of the Au atoms that represent the electrode surface were estimated by using the pathway algorithm developed by Beratan et al.,[48] specifically modified for the present system.[27,39]

Acknowledgements

Financial support by the DFG (Sfb498-A8; PH, D.H.M.), the Fond der Chemischen Industrie (I.M.W.) and the ANPCyT (PICT2006-459; PICT2007-00314) is gratefully acknowledged. M.A.M. and D.H.M. are members of CIC-CONICET. D.F.M. and D.A.P. are CONICET fellows.

Keywords: electron transfer · molecular dynamics · monolayers · proteins · time-resolved spectroscopy

[1] F. A. Armstrong, *Curr. Opin. Chem. Biol.* **2005**, *9*, 110.
[2] D. H. Murgida, P. Hildebrandt, *Chem. Soc. Rev.* **2008**, *37*, 937.
[3] D. H. Murgida, P. Hildebrandt, *Acc. Chem. Res.* **2004**, *37*, 854.
[4] K. K. Chohan, M. Jones, J. G. Grossmann, F. E. Frerman, N. S. Scrutton, M. J. Sutcliffe, *J. Biol. Chem.* **2001**, *276*, 34142.
[5] V. L. Davidson, *Acc. Chem. Res.* **2000**, *33*, 87.
[6] T. Z. Grove, N. M. Kostic, *J. Am. Chem. Soc.* **2003**, *125*, 10598.
[7] L. J. C. Jeuken, *Biochim. Biophys. Acta Bioenerg.* **2003**, *1604*, 67.
[8] S. A. Kang, B. R. Crane, *Proc. Natl. Acad. Sci. USA* **2005**, *102*, 15465.
[9] H. J. Lee, J. Basran, N. S. Scrutton, *Biochemistry* **1998**, *37*, 15513.
[10] H. K. Mei, K. F. Wang, N. Peffer, G. Weatherly, D. S. Cohen, M. Miller, G. Pielak, B. Durham, F. Millett, *Biochemistry* **1999**, *38*, 6846.
[11] F. Millett, B. Durham, *Photosynth. Res.* **2004**, *82*, 1.
[12] J. M. Nocek, S. L. Hatch, J. L. Seifert, G. W. Hunter, D. D. Thomas, B. M. Hoffman, *J. Am. Chem. Soc.* **2002**, *124*, 9404.
[13] J. N. Onuchic, C. Kobayashi, O. Miyashita, P. Jennings, K. K. Baldridge, *Philos. Trans. R. Soc. London Ser. B* **2006**, *361*, 1439.
[14] H. Y. Wang, S. Lin, J. P. Allen, J. C. Williams, S. Blankert, C. Laser, N. W. Woodbury, *Science* **2007**, *316*, 747.
[15] A. V. Zhuravleva, D. M. Korzhnev, E. Kupce, A. S. Arseniev, M. Billeter, V. Y. Orekhov, *J. Mol. Biol.* **2004**, *342*, 1599.
[16] F. A. Armstrong, N. A. Belsey, J. A. Cracknell, G. Goldet, A. Parkin, E. Reisner, K. A. Vincent, A. F. Wait, *Chem. Soc. Rev.* **2009**, *38*, 36.
[17] J. A. Cracknell, K. A. Vincent, F. A. Armstrong, *Chem. Rev.* **2008**, *108*, 2439.
[18] I. Willner, E. Katz, *Angew. Chem.* **2000**, *112*, 1230; *Angew. Chem. Int. Ed.* **2000**, *39*, 1180.
[19] C. E. D. Chidsey, *Science* **1991**, *251*, 919.
[20] R. A. Marcus, *J. Chem. Phys.* **1965**, *43*, 679.
[21] J. Q. Chi, J. D. Zhang, J. E. T. Andersen, J. Ulstrup, *J. Phys. Chem. B* **2001**, *105*, 4669.
[22] K. Fujita, N. Nakamura, H. Ohno, B. S. Leigh, K. Niki, H. B. Gray, J. H. Richards, *J. Am. Chem. Soc.* **2004**, *126*, 13954.
[23] D. H. Murgida, P. Hildebrandt, *J. Am. Chem. Soc.* **2001**, *123*, 4062.
[24] A. Kranich, H. Naumann, F. P. Molina-Heredia, H. J. Moore, T. R. Lee, S. Lecomte, M. A. de La Rosa, P. Hildebrandt, D. H. Murgida, *Phys. Chem. Chem. Phys.* **2009**, *11*, 7390.
[25] P. Zuo, T. Albrecht, P. D. Barker, D. H. Murgida, P. Hildebrandt, *Phys. Chem. Chem. Phys.* **2009**, *11*, 7430.
[26] J. J. Feng, D. H. Murgida, U. Kuhlmann, T. Utesch, M. A. Mroginski, P. Hildebrandt, I. Weidinger, *J. Phys. Chem. B* **2008**, *112*, 15202.
[27] D. A. Paggi, D. F. Martin, A. Kranich, P. Hildebrandt, M. A. Marti, D. H. Murgida, *Electrochim. Acta* **2009**, *54*, 4963.
[28] D. H. Murgida, P. Hildebrandt, *J. Phys. Chem. B* **2002**, *106*, 12814.
[29] L. Rivas, D. H. Murgida, P. Hildebrandt, *J. Phys. Chem. B* **2002**, *106*, 4823.
[30] A. Kranich, H. K. Ly, P. Hildebrandt, D. H. Murgida, *J. Am. Chem. Soc.* **2008**, *130*, 9844.
[31] J. S. Xu, E. F. Bowden, *J. Am. Chem. Soc.* **2006**, *128*, 6813.

[32] K. Niki, W. R. Hardy, M. G. Hill, H. Li, J. R. Sprinkle, E. Margoliash, K. Fujita, R. Tanimura, N. Nakamura, H. Ohno, J. H. Richards, H. B. Gray, *J. Phys. Chem. B* **2003**, *107*, 9947.
[33] A. Avila, B. W. Gregory, K. Niki, T. M. Cotton, *J. Phys. Chem. B* **2000**, *104*, 2759.
[34] A. El Kasmi, J. M. Wallace, E. F. Bowden, S. M. Binet, R. J. Linderman, *J. Am. Chem. Soc.* **1998**, *120*, 225.
[35] H. J. Yue, D. Khoshtariya, D. H. Waldeck, J. Grochol, P. Hildebrandt, D. H. Murgida, *J. Phys. Chem. B* **2006**, *110*, 19906.
[36] J. J. Wei, H. Y. Liu, K. Niki, E. Margoliash, D. H. Waldeck, *J. Phys. Chem. B* **2004**, *108*, 16912.
[37] D. H. Murgida, P. Hildebrandt, J. Wei, Y. F. He, H. Y. Liu, D. H. Waldeck, *J. Phys. Chem. B* **2004**, *108*, 2261.
[38] D. E. Khoshtariya, J. J. Wei, H. Y. Liu, H. J. Yue, D. H. Waldeck, *J. Am. Chem. Soc.* **2003**, *125*, 7704.
[39] D. Alvarez-Paggi, D. F. Martin, P. M. De Biase, P. Hildebrandt, M. A. Marti, D. H. Murgida, unpublished results.
[40] D. H. Murgida, P. Hildebrandt, *J. Phys. Chem. B* **2001**, *105*, 1578.
[41] P. M. De Biase, D. Alvarez-Paggi, F. Doctorovich, P. Hildebrandt, D. A. Estrin, D. H. Murgida, M. A. Marti, *J. Am. Chem. Soc.* **2009**, *131*, 16248.
[42] K. L. Davis, D. H. Waldeck, *J. Phys. Chem. B* **2008**, *112*, 12498.
[43] S. Döpner, P. Hildebrandt, A. G. Mauk, H. Lenk, W. Stempfle, *Spectrochim. Acta Part A* **1996**, *52*, 573.
[44] *Surface-Enhanced Raman Scattering: Physics and Applications* (Eds.: K. Kneipp, H. Kneipp, M. Moskovits), Springer, Berlin, **2006**.
[45] S. Todorovic, C. Jung, P. Hildebrandt, D. H. Murgida, *J. Biol. Inorg. Chem.* **2006**, *11*, 119.
[46] W. Jin, U. Wollenberger, E. Kärgel, W. H. Schunck, F. W. Scheller, *J. Electroanal. Chem.* **1997**, *433*, 135.
[47] B. Michel, H. R. Bosshard, *Biochemistry* **1989**, *28*, 244.
[48] D. N. Beratan, J. N. Onuchic, J. N. Betts, B. E. Bowler, H. B. Gray, *J. Am. Chem. Soc.* **1990**, *112*, 7915.

Received: December 8, 2009
Published online on April 7, 2010

